Supporting information

Windthrows control biomass patterns and functional composition of Amazon forests

Daniel Magnabosco Marra[1,2,3], Susan E. Trumbore[1], Niro Higuchi[2], Gabriel H.P.M. Ribeiro[2], Robinson I. Negrón-Juárez[4], Frederic Holzwarth[3], Sami W. Rifai[5], Joaquim dos Santos[2], Adriano J.N. Lima[2], Valdely F. Kinupp[6], Jeffrey Q. Chambers[4,7] and Christian Wirth[3,8,9]

[1]Biogeochemical Processes Department, Max-Planck-Institute for Biogeochemistry, Jena, Germany; [2]Laboratório de Manejo Florestal, Instituto Nacional de Pesquisas da Amazônia, Manaus, Brazil; [3]AG Spezielle Botanik und Funktionelle Biodiversität, Universität Leipzig, Leipzig, Germany; [4]Climate Sciences Department, Lawrence Berkeley National Laboratory, Berkeley, USA; [5]Environmental Change Institute, Oxford University Centre for the Environment, UK; [6]Instituto Federal de Educação, Ciência e Tecnologia do Amazonas, Campus Manaus-Zona Leste, Herbário EAFM, Av. Cosme Ferreira 8045, São José Operário, 69085-015, Manaus, Brazil; [7]Geography Department, University of California, Berkeley, USA; [8]German Centre for Integrative Biodiversity Research (iDiv) Halle-Jena-Leipzig, Leipzig, Germany; [9]Functional Biogeography Fellow Group, Max-Planck-Institute for Biogeochemistry, Jena, Germany

Correspondence: Daniel Magnabosco Marra, Biogeochemical Processes Department, Max-Planck-Institute for Biogeochemistry, Hans-Knöll-Str. 10, 07745, Jena, Germany. Telephone: +49 3419 738576. Email: dmarra@bgc-jena.mpg.de.

Appendix 1

Study sites

Annual precipitation and temperature in Manaus (Brazil), less than 90 km distant from our study sites, was 2,231 ± 118 mm $year^{-1}$ (mean ± 95% confidence intervals) and 26.9 ± 0.17°C, respectively (period of 1970-2016) (INMET, 2016) (Figure S10). The region has a distinct dry season between July and September with monthly precipitation <100 mm. Windthrows are more frequent between September and February and commonly caused by storm cells embedded in larger and deeper convective systems (Negrón-Juárez et al., 2017).

The terrain at the study sites is undulating. Soils are usually well drained, have low pH and low effective cation exchange (Telles et al., 2003). Plateaus and the upper portions of slopes have high clay content (Oxisols), whereas soils on slope bottoms and valleys have high sand content (Spodosols) (Chauvel, Lucas, & Boulet, 1987). In our *Site 1*, soils from windthrow-affected areas were reported to have higher carbon stocks than those from nearby undisturbed areas, with carbon stocks being positively related to clay content and windthrow tree-mortality (dos Santos et al., 2016).

Fabaceae, Lecythidaceae, Sapotaceae, Chrysobalanaceae and Burseraceae are amongst the botanic families with the highest tree density per hectare in our study region (Chambers et al., 2009; da Silva et al., 2002; Magnabosco Marra et al., 2016; Marra et al., 2014). Tree dominant-height, defined as the average height of 10% of the largest trees, is 30.2 ± 2.9 m (Higuchi, 2015). Nevertheless, some emergent species such as *Dinizia excelsa* Ducke (Fabaceae), *Cariniana decandra* Ducke (Lecythidaceae) and *Caryocar pallidum* A.C. Sm. (Caryocaraceae) can grow to heights of more than 40 m (Ribeiro et al., 1999). Trees larger than 100 cm DBH (diameter at breast height) occur in densities <1 tree ha^{-1} (Vieira et al., 2004) and those with DBH ≤40 cm account for more than 90% of the total density of tress ≥10 cm DBH (da Silva, Martins, Ribeiro, Santos, & Azevedo, 2016).

The *Site 1*, also described in previous studies (dos Santos et al., 2016; Marra et al., 2014; Negrón-Juárez et al., 2018), is located in a large *terra-firme* forest patch accessible from the *Ramal-ZF2* road. A large portion of this area is owned and administered by the *Superintendência da Zona Franca de Manaus* (SUFRAMA). *Site 2* is located *ca*. 35 km north from the *Site 1* in a *terra-firme* forest accessible from the *Ramal-ZF5* road, also owned and administered by the SUFRAMA (Magnabosco Marra, 2016). *Site 3* is located at the *Reserva de Desenvolvimento Sustentável (RDS) do Rio Negro*, a 102,978.83 ha reserve mainly covered by *terra-firme* forests and created in 2008. This area is regulated and protected by the *Centro Estadual de Unidades de Conservação and the Secretaria de Estado do Meio Ambiente e Desenvolvimento Sustentável do Amazonas* (CEUC/SDS), and the *Instituto de Proteção Ambiental do Amazonas* (IPAAM) (Magnabosco Marra, 2016). *Site 4* is covered with old-growth *terra-firme* forest and is located at the *Estação Experimental de Silvicultura Tropical* (EEST), a 21,000 ha reserve (contiguous to *Site 1*) of the *Instituto Nacional de Pesquisas da Amazônia* (INPA). For the *Site 4*, we used data from permanent plots (two transects of 20 m x 2,500 m) installed in 1996 as part of the *Jacaranda Project* (Higuchi et al., 1998). These forest inventory plots are re-measured every one to three years since 1998 by the *Laboratório de Manejo Florestal* (LMF/INPA).

Appendix 2

Detection of windthrows and tree-mortality estimations

Before performing Spectral Mixture Analysis (SMA) (Adams et al., 1995) to account for the windthrow tree-mortality on a per-pixel basis, we first corrected the images for atmospheric 'interferences' and converted it to reflectance using the Atmospheric CORrection Now (ACORN) software (ImSpec LLC, Boulder, CO) (Chambers et al., 2013; Negrón-Juárez et al., 2010). For the required scenes, we applied the Carlotto technique (Carlotto, 1999), which corrects for haze and smoke contamination.

We then calibrated scenes collected prior to the selected windthrows by regressing each band individually against the encoded radiance from the images containing windthrows using temporally invariant targets (Furby & Campbell, 2001). In windthrows, the large amount of non-photosynthetic vegetation (NPV) (i.e. dead vegetation, wood and litter) has high reflectance in Landsat band five (centered at 1.65 μm). This signal is detectable for approximately up to one year, before new leaves obscure litter and dead wood (Chambers et al., 2007; Negrón-Juárez et al., 2010; Nelson et al., 1994).

Further details on the applied methods and routine can be found in previous related studies (Chambers et al., 2007, 2013, Negrón-Juárez et al., 2010, 2011). Satellite imagery processing and SMAs were carried out using the Environment for Visualizing Images software, ENVI (ITT, 2012).

Appendix 3

Botanical surveys and biomass estimation

In our surveys, trees with irregular trunks (e.g. *Protium* spp. and *Eschweilera* spp.), buttresses (e.g. *Sloanea* spp. and *Swartzia* spp.), aerial roots (e.g. *Cecropia* spp. and *Xylopia* spp.), and damaged or wounded trunks were measured above-mentioned irregularities (Clark, 2002). To avoid error in repeated measurements, we marked the height at which diameter measures were taken with paint.

Botanical samples from the wind-disturbed sites were added to the EAFM Herbarium of the *Instituto Federal de Educação, Ciência e Tecnologia do Amazonas, Campus Manaus-Zona Leste* (IFAM-CMZL) (SAWI Project, no. of accession 14,384-15,967) (Magnabosco Marra, 2016). Most samples collected in the *Site 4* containing flowers and/or fruits were added to the INPA Herbarium, while sterile ones were added to the EEST collection (Carneiro et al., 2005; da Silva et al., 2002; Teixeira et al., 2007).

We assessed changes in biomass partitioning among three functional groups of trees: pioneer, mid- and late-successional. This information was compiled from previous studies developed in the Amazon (Amaral et al., 2009; Kammesheidt, 2000; Laurance et al., 2004; Magnabosco Marra et al., 2016) or carried by ourselves taking into account species- or genera-specific traits/attributes and reported demographic patterns (Camargo, Ferraz, Mesquita, Santos, & Brum, 2008; Chazdon, 2014; Clark & Clark, 1992; Laurance et al., 2006; Laurance et al., 2004; Magnabosco Marra et al., 2016; Massoca, Jakovac, Bento, Williamson, & Mesquita, 2012; Saldarriaga, West, Tharp, & Uhl, 1998; Swaine & Whitmore, 1988).

Our biomass estimation models, which have DBH and the species' functional group, DBH and wood density or DBH as a sole predictor (Magnabosco Marra et al., 2016), are adequate to capture the large variations in tree-size distribution and species composition observed in different successional stages, such as in the windthrow chronosequences we

monitored in this study. We employed a complementary allometric model, also adjusted with locally harvested trees (Chambers, Santos, Ribeiro, & Higuchi, 2001), to account for biomass losses from damaged trees, including those having total (i.e. snapped) or partial crown loss. This model has DBH, tree total height (estimated from a DBH:height relationship) and height of failure/breaking as predictors. For these trees, we subtracted the lost biomass from the total estimated biomass.

Appendix 4

Binning approach

Using relatively small subplots (i.e. hundreds of square meters, Table S1) along transects allowed us to more fully account for the gradient of disturbance typical of windthrows and to integrate field and satellite data for estimating the associated tree-mortality at the pixel resolution (30 m x 30 m). This is crucial, since even nearby areas (i.e. side-by-side pixels) can experience different windthrow tree-mortality (Araujo, Nelson, Celes, & Chambers, 2017; Marra et al., 2014; Negrón-Juárez et al., 2011), especially at the periphery of disturbed forest patches.

Meanwhile, reliable biomass estimations in tropical forests require plot sizes that capture environmental and vegetation heterogeneity (Clark & Kellner, 2012; Clark & Clark, 2000; Keller, Palace, & Hurtt, 2001). The increased spatial variations (i.e. within-subplots) on forest structure and floristic composition, typical of windthrown areas (Marra et al., 2014; Rifai et al., 2016), can substantially affect stand-level estimations of biomass (Magnabosco Marra et al., 2016). By binning subplots we aimed at analyzing data over larger areas to obtain more robust and realistic estimates of biomass and community mean wood density. For old-growth forests in our study region, reliable levels of uncertainty on estimates of basal area, which is highly correlated to biomass, can be achieved with plots varying from 800 m^2 to 1200 m^2 (de Oliveira, Higuchi, Celes, & Higuchi, 2014). This is the plot-size range we achieved with our binning approach.

Since we modeled biomass recovery for binned groups, the high biomass stocks that we observed in some disturbed areas (Figs. 2 and S3) may reflect: (*i*) pre-disturbance differences in forest structure that we could not account for (e.g. reflecting the influence of single large trees in a relatively small subplot, *Site 1* and *Site 3*), (*ii*) uncertainties associated with our Landsat-derived estimates of tree-mortality and, (iii) particularly in *Site 3* (late

recovery, 24-27 years since-disturbance), disturbed patches where biomass recovered rapidly exceeding that of undisturbed patches. The higher variation in our response variables and consequent lower r^2-values obtained from our subplot-level analysis (i.e. non-binned data) reflect the greater forest heterogeneity at smaller spatial scales.

Appendix 5

Calculations of community mean wood density and predictions of tree annual-growth

Community mean wood density was calculated as the abundance weighted-mean wood density of trees recorded in a given subplot. For species where more than one wood density value was found, we used the mean value. For species where no published data was available or where the identification was carried out to the genus level (~45% of the total recorded species), we used the mean wood density for all species from the same genus reported as occurring in Central Amazon. For trees identified only to the family level (~12%), we used the mean value of genera belonging to that family and reported as occurring in Central Amazon. For 11 unidentified trees we did not assign functional group nor wood density values and used the model with DBH as the sole predictor for the estimation of biomass.

To fit random forest models for predicting the DBH of recruits backwards, we selected trees from *Sites 1-3*, for which we had two or three consecutive DBH measures and could calculate annual growth rates (n=8984). From these, we randomly selected a data set (n=4,000) to train prediction models and another data set (n=999) to evaluate their predictive performance. We fit models with varying sets of predictors using *ntree*=2,000 and *mtry*=3 (Breiman, 2001). For the final two models we selected the fewest number of predictors (i.e. DBH, wood density, species' successional group, elevation, windthrow tree-mortality, time since disturbance) yielding the highest coefficient of determination (r^2_{adj}) and the lowest adjusted root mean squared error (RMSE) for calibration and validation fits. The final two models we applied (with and without wood density as predictor) had calibration and validation r^2_{adj} from 0.37-0.47 and RMSE from 1.1-2.2 cm $year^{-1}$ (Figure S2 and Table S2).

Appendix 6

Data analysis

To examine patterns of biomass and its components we fitted *generalized additive models* (GAMs) (Hastie & Tibshirani, 1987, 1990). GAMs are a non-parametric extension of generalized linear models, with a penalized polynomial structure defined by unspecified functions (linear and non-linear) that are estimated iteratively (Hastie & Tibshirani, 1990; Wood, 2006). We fit a series of models with a varying number of *knots* (k) for explanatory variables following a standard routine to evaluate significance of smooth terms, effective degrees of freedom and models' deviance (Wood, 2006). We finally fixed k=3 since this value yielded models that minimized residual deviance and maximized parsimony. Apart from checking the 95% confidence intervals using standard errors from predictions, we checked the influence of data skewness by employing a bootstrap procedure. We sampled plots randomly from our entire data set (1,000 replicates) and quantified non-parametric 95% confidence intervals from the Bayesian posterior covariance-matrix of parameters. This procedure produced very similar results (not presented) supporting that the main variations in our data set were captured by GAMs. The model describing relative biomass stocks produced skewed residual distributions due to the effect of windthrow-affected areas showing greater biomass stocks than the areas assumed as undisturbed (Figures 2 and S3). As discussed in the main text and in the Appendix 4, we attribute these to intrinsic landscape variation in forest biomass, such as the occurrence of rare large-trees (da Silva et al., 2016; Vieira et al., 2004) in specific subplots or possible misclassification of our remote-sensing approach.

The processing statistical analyses on the vegetation were carried out in the R 3.4.2 software platform (R Team, 2015). GAMs and random forest regression models were fit following standard routine available in the packages *mgcv* (Wood, 2006) and *RandomForest*

(Liaw & Wiener, 2002), respectively. R codes were self-written and figures produced by using standard functions and the *ggplot2* package (Wickham, 2009).

AUTHOR CONTRIBUTIONS

DMM, SET, NH, JQC and CW designed research; DMM, GHPMR, AJNL, SWR and RINJ performed research; FH and VFK contributed analytic tools; DMM analyzed data; DMM, SET and CW wrote the paper; GHPMR, RINJ, FH and SWR assisted with editing the paper

REFERENCES

Adams, J. B., Sabol, D. E., Kapos, V., Filho, R. A., Roberts, D., Smith, M. O., & Gillespie, A. R. (1995). Classification of multispectral images based on fractions of endmembers: Application to land-cover change in the Brazilian Amazon. *Remote Sensing of Environment*, *52*, 137–154.

Amaral, D. D., Vieira, I. C. G., Almeida, S. S., Salomão, R. P., Silva, A. S. L., & Jardim, M. A. G. (2009). Checklist of remnant forest fragments of the metropolitan area of Belém and historical value of the fragments, State of Pará, Brazil. *Bol. Mus. Para. Emílio Goeldi*, *4*(3), 231–289.

Araujo, R. F., Nelson, B. W., Celes, C. H. S., & Chambers, J. Q. (2017). Regional distribution of large blowdown patches across Amazonia in 2005 caused by a single convective squall line. *Geophysical Research Letters*, *44*, 1–6.

Breiman, L. (2001). Random forests. *Machine Learning*, *45*(1), 5–32.

Camargo, J. L. C., Ferraz, I. D. K., Mesquita, M. R., Santos, B. A., & Brum, H. D. (2008). *Guia de Propágulos & Plântulas da Amazônia vol.1*. (Authors, Ed.) (1st ed.). Manaus: INPA.

Carlotto, M. J. (1999). Reducing the effects of space-varying, wavelength-dependent scattering in multispectral imagery. *International Journal of Remote Sensing*, *20*, 3333–3344.

Carneiro, V. C. M., Higuchi, N., Santos, J. dos, Pinto, A. C. M., Teixeira, L. M., Lima, A. J. N., … Rocha, R. de M. (2005). *Composição Florística e Análise Estrutural da Floresta de Terra Firme na Região de Manaus, Estado do Amazonas, Brasil*. *Actas das Comunicações - Inventário, Modelação e Gestão*. Viso, Portugal: V Congresso Florestal Nacional A Floresta e as Gentes. Retrieved from http://www.esac.pt/cernas/cfn5/docs/T2-40.pdf

Chambers, J. Q., Asner, G. P., Morton, D. C., Anderson, L. O., Saatchi, S. S., Espírito-Santo, F. D. B., … Souza Jr, C. (2007). Regional ecosystem structure and function: ecological insights from remote sensing of tropical forests. *Trends in Ecology & Evolution*, *22*(8), 414–423.

Chambers, J. Q., Negron-Juarez, R. I., Marra, D. M., Di Vittorio, A., Tews, J., Roberts, D., … Higuchi, N. (2013). The steady-state mosaic of disturbance and succession across an old-growth Central Amazon forest landscape. *Proceedings of the National Academy of Sciences of the United States of America*, *110*(10), 3949–3954.

Chambers, J. Q., Robertson, A. L., Carneiro, V. M. C., Lima, A. J. N., Smith, M. L., Plourde, L. C., & Higuchi, N. (2009). Hyperspectral remote detection of niche partitioning among canopy trees driven by blowdown gap disturbances in the Central Amazon. *Oecologia*, *160*(1), 107–117.

Chambers, J. Q., Santos, J. dos, Ribeiro, R. J., & Higuchi, N. (2001). Tree damage, allometric relationships, and above-ground net primary production in central Amazon forest. *Forest Ecology and Management*, *152*(1–3), 73–84.

Chauvel, A., Lucas, Y., & Boulet, R. (1987). On the genesis of the soil mantle of the region of Manaus, Central Amazonia, Brazil. *Experientia*, *43*, 234–241.

Chazdon, R. (2014). *Second Growth: The Promise of Tropical Forest Regeneration in an Age of Deforestation*. Chicago, IL: University of Chicago Press.

Clark, D. A. (2002). Are tropical forests an important carbon sink? Reanalysis of the long-term plot data. *Ecological Applications*, *12*(1), 3–7.

Clark, D. A., & Clark, D. B. (1992). Life history diversity of canopy and emergent trees in a neotropical rain forest. *Ecological Monographs*, *62*(3), 315–344.

Clark, D. B., & Kellner, J. R. (2012). Tropical forest biomass estimation and the fallacy of misplaced concreteness. *Journal of Vegetation Science*, *23*(6), 1191-1196.

Clark, D., & Clark, D. (2000). Landscape-scale variation in forest structure and biomass in a tropical rain forest. *Forest Ecology and Management*, *137*(1–3), 185–198.

da Silva, K. E., Martins, S. V, Ribeiro, C. A. A., Santos, N. T., & Azevedo, C. P. (2016). Structure of 15 hectares permanent plots of Terra Firme dense forest in central Amazon. *Revista Árvore*, *40*, 603–615.

da Silva, R. P., dos Santos, J., Tribuzy, E. S., Chambers, J. Q., Nakamura, S., & Higuchi, N. (2002). Diameter increment and growth patterns for individual tree growing in Central Amazon, Brazil. *Forest Ecology and Management*, *166*(1–3), 295–301.

de Oliveira, M., Higuchi, N., Celes, C., & Higuchi, F. (2014). Size of plots and forms for forest inventory of tree species in Central Amazon. *Ciência Florestal*, *24*(3), 645–653.

dos Santos, L. T., Magnabosco Marra, D., Trumbore, S., De Camargo, P. B., Negrón-Juárez, R. I., Lima, A. J. N., … Higuchi, N. (2016). Windthrows increase soil carbon stocks in a central Amazon forest. *Biogeosciences*, *13*(4), 1299–1308. http://doi.org/10.5194/bg-13-1299-2016

Furby, S. L., & Campbell, N. A. (2001). Calibrating images fromdifferent dates to "like-value" digital counts. Remote Sensing of Environment. *Remote Sensing of Environment*, *77*, 186–196.

Hastie, T. J. T., & Tibshirani, R. J. (1990). *Generalized Additive Models*. *Statistics* (Vol. 1). New York: Chapman and Hall/CRC.

Hastie, T., & Tibshirani, R. (1987). Generalized Additive Models: Some Applications. *Journal of the American Statistical Association*, *82*(398), 371–386.

Higuchi, F. G. (2015). *Dinâmica de volume e biomassa da floresta de terra firme do Amazonas*. PhD thesis, University of Paraná, Brazil, 201p.

Higuchi, N., Santos, J. dos, Vieira, G., Ribeiro, R. J., Sakurai, S., Ishizuka, M., … Saito, S. (1998). Análise estrutural da floresta primária da bacia do rio Cuieiras, ZF-2, Manaus-AM, Brasil. In N. Higuchi, M. A. A. Campos, P. T. B. Sampaio, & J. dos Santos (Eds.), *Pesquisas Florestais para Conservação da Floresta e Reabilitaçao de Áreas Degradadas da Amazônia* (pp. 51–81). Manaus: Instituto Nacional de Pesquisas da Amazônia (INPA).

INMET. (2016). Instituto Nacional de Metereologia (INMET). Retrieved from http://www.inmet.gov.br/

ITT. (2012). Environment for Visualizing Images software (ENVI). Boulder, CO, USA.

Kammesheidt, L. (2000). Some autecological characteristics of early to late successional tree species in Venezuela. *Acta Oecologica*, *21*(1), 37–48.

Keller, M., Palace, M., & Hurtt, G. (2001). Biomass estimation in the Tapajos National Forest, Brazil. *Forest Ecology and Management*, *154*(3), 371–382.

Laurance, W. F., Nascimento, H. E. M., Laurance, S. G., Condit, R., D'Angelo, S., &

Andrade, A. (2004). Inferred longevity of Amazonian rainforest trees based on a long-term demographic study. *Forest Ecology and Management*, *190*(2–3), 131–143.

Laurance, W., Nascimento, H., Laurance, S., Andrade, A., Fearnside, P., Ribeiro, J., & Capretz, R. (2006). Rain forest fragmentation and the proliferation of successional trees. *Ecology*, *87*(2), 469–482.

Liaw, A., & Wiener, M. (2002). Classification and Regression by randomForest. *R News*, *2*(3), 18–22.

Magnabosco Marra, D. (2016). *Effects of windthrows on the interaction between tree species composition, forest dynamics and carbon balance in Central Amazon*. PhD thesis, University of Leipzig, Germany, 256p.

Magnabosco Marra, D., Higuchi, N., Trumbore, S. S. E., Ribeiro, G. H. P. M. G., Dos Santos, J., Carneiro, V. M. C. V., … Wirth, C. (2016). Predicting biomass of hyperdiverse and structurally complex central Amazonian forests - A virtual approach using extensive field data. *Biogeosciences*, *13*(5), 1553–1570.

Marra, D., Chambers, J., Higuchi, N., Trumbore, S., Ribeiro, G., Dos Santos, J., … Wirth, C. (2014). Large-scale wind disturbances promote tree diversity in a central Amazon forest. *PLoS ONE*, *9*(8), e103711–e103711.

Massoca, P. E. S., Jakovac, A. C. C., Bento, T. V, Williamson, G. B., & Mesquita, R. C. G. (2012). Dynamics and trajectories of secondary succession in Central Amazonia. *Bol. Mus. Para. Emílio Goeldi*, *7*(3), 235–250.

Negrón-Juárez, R. I., Chambers, J. Q., Guimaraes, G., Zeng, H., Raupp, C. F. M., Marra, D. M., … Higuchi, N. (2010). Widespread Amazon forest tree mortality from a single cross-basin squall line event. *Geophysical Research Letters*, *37*(16), 1–5.

Negrón-Juárez, R. I., Chambers, J. Q., Marra, D. M., Ribeiro, G. H. P. M., Rifai, S. W., Higuchi, N., & Roberts, D. (2011). Detection of subpixel treefall gaps with Landsat imagery in Central Amazon forests. *Remote Sensing of Environment*, *115*(12), 3322–3328.

Negrón-Juárez, R. I., Holm, J., Magnabosco Marra, D., Rifai, S., Riley, W., Chambers, J., … Higuchi, N. (2018). Vulnerability of Amazon forests to storm-driven tree mortality. *Environmental Research Letters*, *13*(5), 54021.

Negrón-Juárez, R. I., Jenkins, H. S., Raupp, C. F. M., Riley, W. J., Kueppers, L. M., Marra, D. M., … Higuchi, N. (2017). Windthrow Variability in Central Amazonia. *Atmosphere*, *8*(2), 28.

Nelson, B., Kapos, V., Adams, J., Oliveira, W., Braun, O., & do Amaral, I. (1994). Forest disturbance by large blowdowns in the Brazilian Amazon. *Ecology*, *75*(3), 853–858.

Ribeiro, J. E. L. S., Hopkins, M. J. G., Vicentini, A., Sothers, C. A., Costa, M. A. da S., Brito, J. M. de, … Procópio, L. C. (1999). *Flora da Reserva Ducke: Guia de Identificação das Plantas Vasculares de uma Floresta de Terra-firme na Amazônia Central*. Manaus: INPA.

Rifai, S. W., Urquiza Muñoz, J. D., Negrón-Juárez, R. I., Ramírez Arévalo, F. R., Tello-Espinoza, R., Vanderwel, M. C., … Bohlman, S. A. (2016). Landscape-scale consequences of differential tree mortality from catastrophic wind disturbance in the Amazon. *Ecological Applications*, *26*(7), 2225–2237.

R Development Core Team (2015). R: A language and environment for statistical computing.

Vienna, Austria: R Foundation for Statistical Computing. Retrieved from http://www.r-project.org

Saldarriaga, J. G., West, D. C., Tharp, M. L., & Uhl, C. (1998). Long-Term Chronossequence of Forest Succession in the Upper Rio Negro of Colombia and Venezuela. *Journal of Ecology*, *76*, 938–958.

Scott, D. W. (2015). *Multivariate density estimation: theory, practice, and visualization* (2nd ed.). John Wiley & Sons, Inc.

Swaine, M. D., & Whitmore, T. C. (1988). On the definition of ecological species groups in tropical rain forests. *Vegetatio*, *75*(1–2), 81–86.

Teixeira, L. M., Chambers, J. Q., Silva, A., Lima, A. J. N., Carneiro, V. M. C., Santos, J. dos, & Higuchi, N. (2007). Projeção da dinâmica da floresta natural de Terra- firme , região de Manaus-AM , com o uso da cadeia de transição probabilística de Markov. *Acta Amazonica*, *37*(3), 377–384.

Telles, E. C., Camargo, P. B., Martinelli, L. A., Trumbore, S. E., Costa, E. S., Santos, J., … Oliveira Jr, C. (2003). Influence of soil texture on carbon dynamics and storage potential in tropical forest soils of Amazonia. *Global Biogeochemical Cycles*, *17*(2), 1–12.

Vieira, S., de Camargo, P. B., Selhorst, D., da Silva, R., Hutyra, L., Chambers, J. Q., … Martinelli, L. A. (2004). Forest structure and carbon dynamics in Amazonian tropical rain forests. *Oecologia*, *140*(3), 468–479.

Wickham, H. (2009). *ggplot2: elegant graphics for data analysis*. Springer New York.

Wood, S. N. (2006). *Generalized Additive Models: an introduction with R*. Boca Raton: Chapman and Hall/CRC.

TABLES

Table S1 Study sites comprising an old growth and wind-disturbed *terra-firme* forests in Central Amazon, Brazil

Site	Coordinates	Yd	Fi	Nt	Ns	Dim	Area	Elev	Ws	M
1	2°33'43" S 60°16'00" W	2005	2009, 2012 and 2015	2 (100), 2 (600) and 2 (1000)	72	10 x 25	1.8	(57, 78, 117)	Undisturbed/control	≤4 (0, 0.7, 3.9)
					28	10 x 25	0.7	(61, 89, 117)	Low	4-20 (4.7, 12.3, 19.7)
					30	10 x 25	0.75	(49, 85, 117)	Moderate	20-40 (20.1, 27.5, 39.7)
					14	10 x 25	0.35	(60, 81, 112)	High	>40 (40.9, 53.7, 69.7)
2	2°15'09" S 60°10'24" W	1996	2010, 2013 and 2016	1 (3000)	21	10 x 30	0.63	(86, 100, 111)	Undisturbed/control	≤4 (0, 0.5, 3.9)
					37	10 x 30	1.11	(86, 101, 117)	Low	4-20 (4.7, 11, 19)
					19	10 x 30	0.57	(92, 105, 116)	Moderate	20-40 (21.4, 31.8, 39.9)
					23	10 x 30	0.69	(94, 100, 119)	High	>40 (40.3, 48, 57)
3	3°00'00" S 60°45'11" W	1987	2011 and 2014	2 (1500)	49	10 x 30	1.47	(40, 66, 78)	Undisturbed/control	≤4 (0, 0.2, 2.6)
					13	10 x 30	0.39	(54, 70, 75)	Low	4-20 (6.2, 12.2, 19.2)
					28	10 x 30	0.84	(50, 68, 75)	Moderate	20-40 (20.5, 30.1, 39.1)
					10	10 x 30	0.3	(60, 69, 74)	High	>40 (40.2, 47.1, 56.2)
4	2°36'40" S 60°12'10" W	-	2002 and 2004	2 (2500)	250	20 x 20	10	(61, 94, 123)	Undisturbed/control	

Note. Yd- year of windthrow; Fi- years in which forest-inventories were carried; Nt- number and length (m; in parenthesis) of transects; Ns- number of monitored subplots; Dim- subplots' dimensions (m); Area- total sampled area (ha); Elev- subplot elevation (m) (minimum, mean and maximum, respectively) extracted from a digital elevation model with a 30 m x 30 m spatial-resolution (Shuttle Radar Topographic Mission *SRTM*); Ws- windthrow severity; and M- windthrow tree-mortality (%) (minimum, mean and maximum, respectively)

Table S2 Goodness of fit of *random forest algorithms* used to predict annual growth in DBH for individual trees in Central Amazon forests. The data set used to calibrate and validate the models includes old growth and wind-disturbed forests (Figure 1 and Table S1)

Model	Predictors	Calibration (n=4000)			Validation (n=999)		
		r^2_{adj}	RMSE	Predicted annual growth	r^2_{adj}	RSME	Predicted annual growth
1	DBH, wood density, species' successional group, elevation, windthrow tree-mortality, time since disturbance	0.448	1.065	(-0.126, 0.247, 2.048)	0.469	2.074	(-0.333, 0.272, 2.867)
2	DBH, species' successional group, elevation, windthrow tree-mortality, time since disturbance	0.370	1.141	(-0.115, 0.246, 1.744)	0.383	2.231	(-0.034, 0.262, 1.857)

Note. Minimum, mean and maximum annual growth of trees from the calibration data set was -0.733 cm, 0.248 cm and 4.5 cm, respectively. DBH- diameter at breast height (1.3 m); r^2_{adj}- adjusted coefficient of determination; RMSE- root mean squared error; and Predicted annual growth (minimum, mean and maximum, respectively)

Table S3 Summary of fitting measures of *generalized additive models* explaining changes in relative biomass stock (Rel bio), biomass increment (Bio incr) and loss (Bio loss), net biomass change (Net bio) and relative wood density (Rel WD) in Central Amazon forests, Brazil. The data set used to fit the models includes an old growth and three other forests that experienced a wide gradient of windthrow tree-mortality and that span 4-27 years of recovery (Figure 1 and Table S1). *Rel bio* and *Rel WD* were calculated as relative to the undisturbed chronosequence in the same time period. Here, we analyzed data at subplot level to test for possible effects of terrain elevation on our response variables. We also checked for possible spatial autocorrelation due to subplots nested in transects (Appendix 1), which could bias the results from models fit with binned data

						Smooth terms					
	Df	r^2_{adj}	Dev	GCV	Parametric coefficient Intercept (error)	T Edf (F)	M Edf (F)	M:T Edf (F)	Subplots/ transects Edf (F)	M:Elev Edf (F)	Elev:Site Edf (F)
Rel bio	929	0.083	8.6	91.7	0.189 (0.009)***	0.774 (507.9)***	1 (38.2)***	1.997 (915.4)***			
	928	0.094	9.8	90.7	0.228 (0.014)	1.293 (133.9)***	1 (24.2)***	1.997 (354.4)***	0.961 (7.2)***		
	926	0.135	14.3	87.1	-0.184 (0.062)**	0.774 (11.3)**	1.837 (2.3)	2.611 (4.9)**	0.462 (0.8)	2 (20.9)***	2 (13.4)***
Bio incr	585	0.055	6	1271.8	0.889 (0.043)***	0.783 (524.3)***	1 (23.1)***	2.494 (632.4)***			
	584	0.055	6	1271.8	0.889 (0.043)***	0.783 (524.3)***	1 (23.1)***	2.494 (632.4)***	<0.001 (0)		
	582	0.111	12.6	1209.3	-0.696 (0.303)*	0.945 (4.5)*	1 (8.5)**	2.839 (2.6)*	0.847 (4.2)*	2.898 (11.8)***	2 (14.6)***
Bio loss	585	0.002	0.8	15477	-0.768 (0.150)***	0.782 (32.5)***	1.717 (1.5)	1.997 (22.7)***			
	584	0.002	0.8	15477	-0.768 (0.150)	0.782 (32.5)***	1.717 (1.5)	1.997 (22.7)***	<0.001 (0)		
	582	0.022	3.7	15299	1.273 (1.043)	1.64 (3.2)*	1 (0.1)	1.997 (0.1)	0.529 (1)	2.565 (2.1)	2 (2.4)$^{¥}$
Net bio	585	0.002	0.8	16554	0.123 (0.155)	0.783 (0.7)	1.6 (0.8)	1.996 (10.2)***			
	584	0.002	0.8	16554	0.123 (0.155)	0.783 (0.7)	1.6 (0.8)	1.996 (10.2)***	<0.001 (0)		
	582	0.009	2.5	16604	0.523 (0.994)	1.556 (1.8)	1.426 (1.5)	1.996 (0.2)	<0.001 (0)	3 (1)	2 (0.8)
Rel WD	929	0.325	32.9	1.469	0.224 (0.001)***	1.724 (12618)***	1.92 (12)***	2.991 (43198)***			
	928	0.331	33.6	1.457	0.228 (0.002)***	1.633 (6871.3)***	1.946 (9.8)***	2.98 (14281.2)***	0.86 (5.7)**		
	926	0.358	36.6	1.406	0.202 (0.009)***	1.71 (276.8)***	2 (6.2)**	2.9 (119.6)***	0.864 (6.9)**	2.549 (4.1)**	2.716 (1.3)

Note. Df- degrees of freedom; r^2_{adj}- adjusted coefficient of determination; Dev- models' deviance/quality-of-fit (%); GCV- generalized cross validation; Edf- estimated degrees of freedom; T- time since disturbance (years); M- windthrow tree-mortality. Significance based on Wald tests: $^{¥}$p <0.1; *p <0.05; **p <0.01; ***p <0.001

Table S4 Summary of fitting measures of *generalized additive models* explaining changes in relative biomass stock (Rel bio), biomass increment (Bio incr) and loss (Bio loss), net biomass change (Net bio) and relative wood density (Rel WD) in Central Amazon forests, Brazil. The data set used to fit the models includes an old growth and three other forests that experienced a wide gradient of windthrow tree-mortality and that span 4-27 years of recovery (Figure 1 and Table S1). *Rel bio* and *Rel WD* were calculated as relative to the undisturbed chronosequence in the same time period. Results from equivalent models fit with plot-biomass data estimated with allometric models relying on different predictors (i.e. DHB + wood density and DBH solely) indicated that the patterns we detected are consistent when using other allometries

						Smooth terms				
					Parametric coefficient	T	M	M:T	M:Elev	Elev:Site
	Df	r^2_{adj}	Dev	GCV	Intercept (error)	Edf (F)	Edf (F)	Edf (F)	Edf (F)	Edf (F)
Tree biomass estimated with DBH + species' functional group										
Rel bio	171	0.387	41.8	0.045	0.121 (0.007)***	0.826 (317.8)***	1 (52.8)***	1.997 (847.8)***		
	169	0.401	44.2	0.045	0.049 (0.033)	1.483 (2.8)*	1 (4.2)*	1.997 (11.3)***	2 (3)$^{¥}$	0.713 (2.2)$^{¥}$
Bio incr	107	0.214	25.9	0.877	0.759 (0.039)***	0.836 (436.4)***	1 (23.1)***	2.354 (629.1)***		
	106	0.256	31.8	0.854	0.373 (0.182)*	0.836 (4.7)$^{¥}$	1 (0.7)	2.504 (19.8)***	2 (2.9)$^{¥}$	0.874 (6.9)**
Bio loss	107	0.01	4.5	11.296	-0.645 (0.142)***	0.836 (23.9)***	1.712 (1.51)	1.996 (24.7)***		
	106	0.027	8.9	11.438	0.558 (0.794)	1.308 (0.3)	1.618 (0.8)	1.996 (0)	2 (1.4)	0.716 (2.5)$^{¥}$
Net bio	107	0.017	5	11.1	0.119 (0.141)	0.836 (0.8)	1.658 (1.1)	1.996 (8.7)***		
	106	0.005	5.9	11.5	0.267 (0.531)	0.931 (0.2)	1.679 (1)	1.996 (0.4)	2 (0.1)	0.164 (0.2)
Rel WD	171	0.641	68	0.001	0.171 (0.001)***	1.734 (7330.6)***	1.877 (8.1)***	2.957 (25250.4)***		
	169	0.646	68.8	0.001	0.164 (0.006)***	1.737 (673.3)***	1.794 (2)	2.997 ((380.4)***	2 (2)	<0.001 (0)
Tree biomass estimated with DBH + wood density										
Rel bio	171	0.423	45.5	0.033	0.118 (0.006)***	0.826 (413)***	1 (67.9)***	1.997 (1197.7)***		
	169	0.441	48.5	0.033	0.048 (0.03)	1.654 (5.9)**	1.394 (4.4)*	1.997 (17.3)***	2 (3.5)*	0.791 (3.3)*
Bio incr	107	0.378	42.3	0.918	0.716 (0.04)***	0.836 (370.8)***	1 (27.1)***	1.996 (823.9)***		
	106	0.41	46.7	0.895	0.26 (0.183)	0.836 (2.2)	1 (<0.1)	1.996 (17.1)***	2 (3.8)*	0.825 (4.7)*
Bio loss	107	0.022	6	8.7	-0.588 (0.125)***	1.109 (18.4)***	1.764 (1.77)	1.996 (27.6)***		
	106	0.033	9.6	8.8	0.485 (0.722)	1.438 (0.5)	1.642 (0.9)	1.996 (<0.1)	2 (1.3)	0.655 (1.9)$^{¥}$
Net bio	107	0.07	10.7	8.8	0.134 (0.126)	1.214 (0.4)	1.754 (2)	1.996 (14.9)***		
	106	0.06	11.2	9.1	0.235 (0.542)	1.236 (0.2)	1.693 (1.1)	1.996 (0.4)	2 (<0.1)	<0.001 (0)

Tree biomass estimated with DBH solely

Rel bio	171	0.38	40.6	0.032	0.118 (0.006)***	0.826 (415.7)***	1 (71.8)***	1.997 (1405.6)***		
	169	0.392	42.8	0.032	0.056 (0.028)$^{¥}$	1.46 (3.5)*	1 (9)**	1.997 (27.5)***	2 (2.7)$^{¥}$	0.74 (2.5)$^{¥}$
Bio incr	107	0.524	56.7	0.822	0.666 (0.038)***	0.836 (356.2)***	1 (39.7)***	2.318 (635.3)***		
	106	0.556	61.2	0.8	0.281 (0.175)	0.836 (2.7)	1.759 (1.5)	2.996 (14.3)***	2 (3.8)*	0.798 (3.5)*
Bio loss	107	0.014	5.1	5.5	-0. 447 (0.098)***	0.913 (20.2)***	1.721 (1.4)	1.996 (36.3)***		
	106	0.034	9.7	5.5	0.478 (0.568)	1.383 (0.4)	1.612 (0.8)	1.996 (0.1)	2 (1.6)	0.721 (2.6)$^{¥}$
Net bio	107	0.094	13.3	5.7	0.225 (0.1)*	1.071 (3.1)$^{¥}$	1.662 (2.6)$^{¥}$	1.996 (23.7)***		
	106	0.087	14.4	5.8	0.57 (0.477)	1.349 (1.1)	1.516 (0.5)	1.996 (1.3)	2 (0.2)	0.093 (0.1)

Note. Df- degrees of freedom; r^2_{adj}- adjusted coefficient of determination; Dev- models' deviance/quality-of-fit (%); GCV- generalized cross validation; Edf- effective degrees of freedom; T- time since disturbance (years); M- windthrow tree-mortality (%). Significance based on Wald tests: $^{¥}p < 0.1$; $^{*}p < 0.05$; $^{**}p < 0.01$; $^{***}p < 0.001$. *Elevation* and *Sites* were not included in our final models for predictions of biomass and community mean wood-density patterns (Figures 2-4 and 6)

Table S5 Time to recover at least 90% of reference biomass stocks following different windthrow tree-mortality in Central Amazon forests, Brazil. Predictions were made with different *generalized additive models* (GAMs) fit with plot-biomass data estimated with allometric models relying on different predictors

Biomass predictors	Windthrow tree-mortality (%)	Relative biomass stock	Time since disturbance (years)
DBH + species' functional group	20	0.9 ± 0.06	27
	40	0.91 ± 0.16	37
	65	0.92 ± 0.32	40
DBH + wood density		0.9 ± 0.4	23
		0.9 ± 0.11	31
		0.9 ± 0.22	34
DBH		0.91 ± 0.3	17
		0.91 ± 0.06	23
		0.9 ± 0.13	25

FIGURES

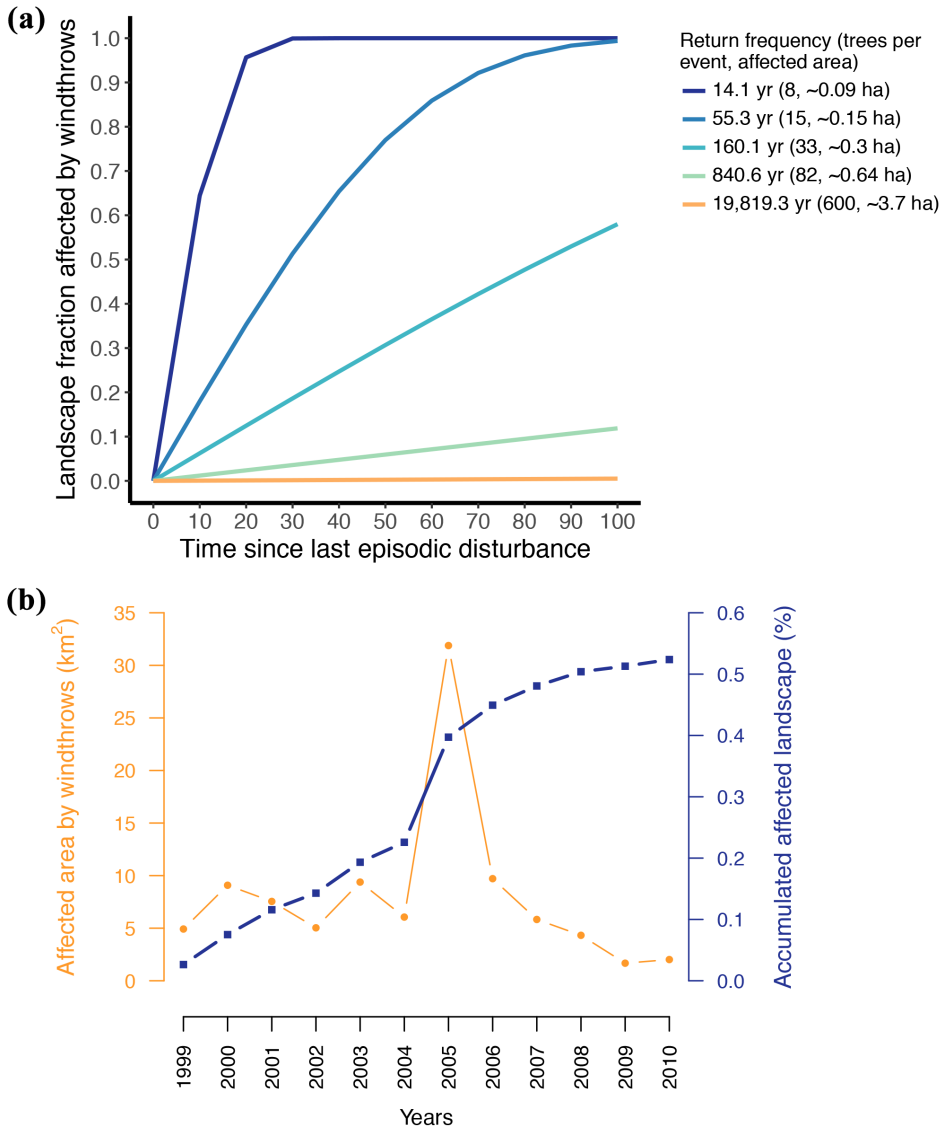

Figure S1 Windthrow affected-area in Central Amazon, including our study region: (a) hectare-scale return-frequency of windthrows and predicted affected-area, and (b) windthrow affected-area in Central Amazon over a 12year-interval. Data on the size-frequency distribution of windthrows, number of dead trees and total affected-area were compiled from a regional assessment that integrates field plot-data, remote sensing disturbance probability distribution functions and individual-based simulation modeling (TRECOS) (Chambers *et al.*, 2013, Figure 4). Annual estimates of the windthrow affected-area were carried out on a chronosequence (1999-2010) of Landsat images (p231, r062) covering the region of Manaus (~18,609 km^2) (INPE, 2016) and account for windthrows >5 ha (Negrón-Juárez *et al.*, 2017)

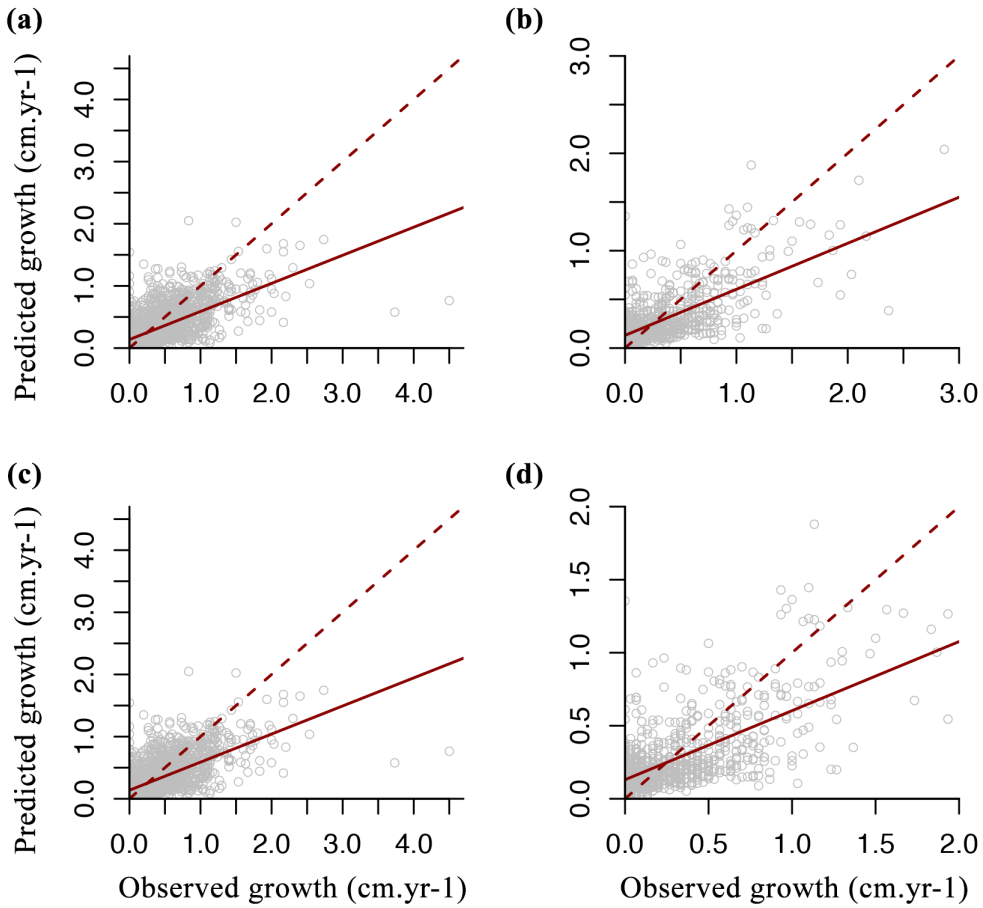

Figure S2 Random forest models used to predict annual growth in DBH for trees in Central Amazon forests. Relationship between predicted and observed growth rates for the (*a* and *c*) calibration (n=4000) and (*b* and *d*) validation (n=999) of two different models, with (*a* and *b*) and without (*c* and *d*) wood density as predictors. The data set used to fit the models includes trees growing in old growth and windthrown forests spanning a wide gradient of windthrow tree-mortality and 4-27 years of recovery

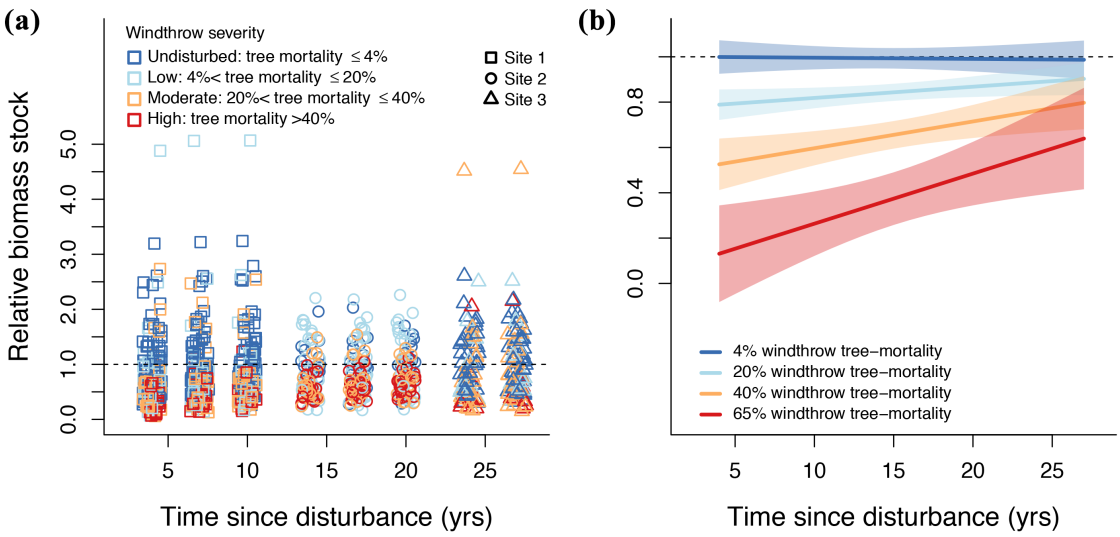

Figure S3 Biomass recovery in wind-disturbed forests in Central Amazon, Brazil: (a) observed relative biomass stocks (i.e. compared to the mean biomass stocks of undisturbed forest patches in the same time period, dark-blue points) and (b) predicted biomass recovery over time since disturbance for different windthrow severities. Predictions were made with *generalized additive models* (GAMs) fit on subplot-level data on time since disturbance and windthrow tree-mortality (and their interaction) as predictors (Table S3). In panel *a*, we jittered data points to reduce overlap. Dark-blue points are mean values of relative biomass in undisturbed chronosequences. Shaded areas indicate the 95% confidence intervals of predictions

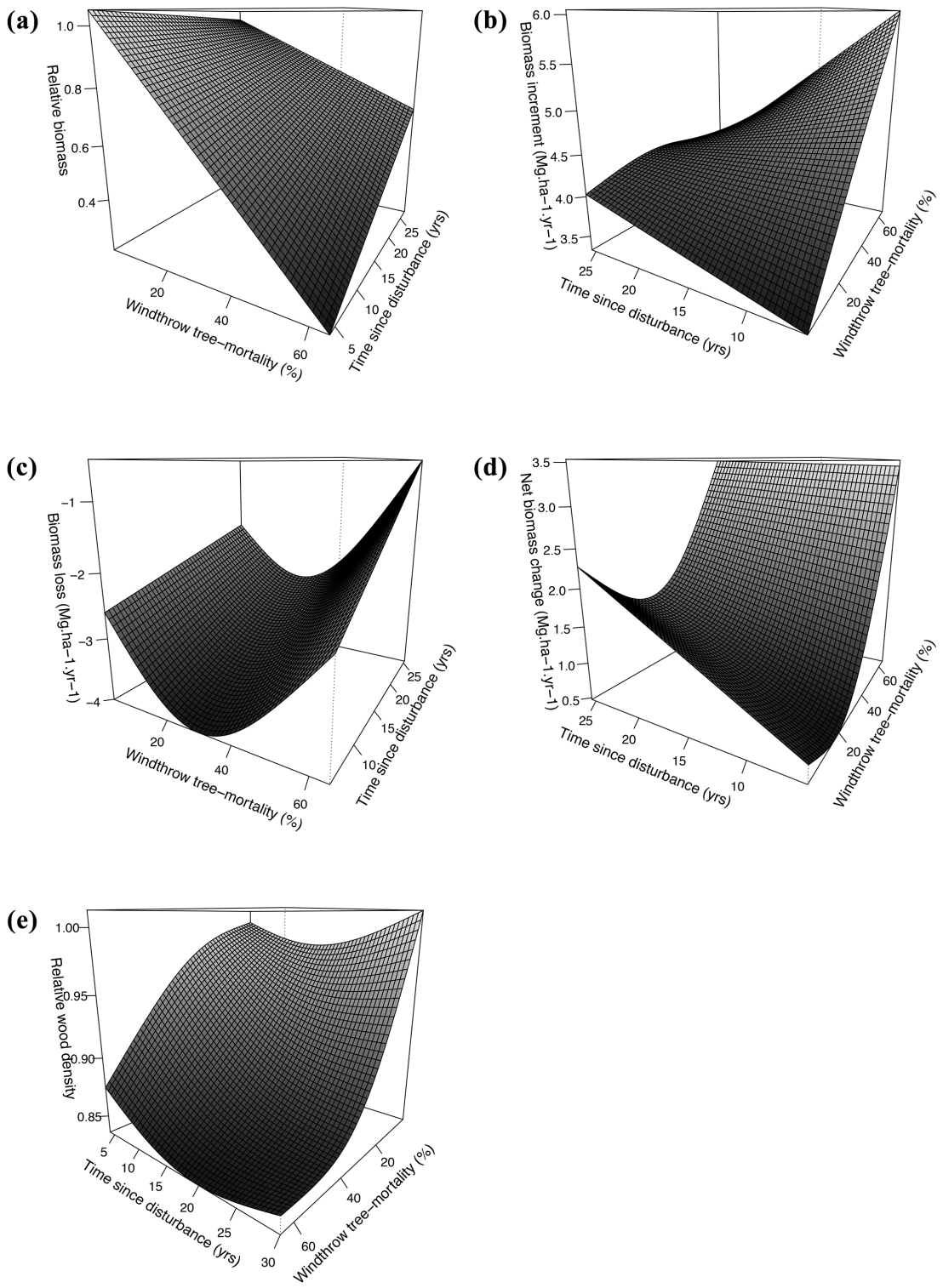

Figure S4 *Generalized additive models* (GAMs) with time since disturbance and windthrow tree-mortality (and their interaction) as predictors of biomass recovery and its components in Central Amazon forests, Brazil: (a) relative biomass stock, (b) biomass increment and (c) loss, (d) net biomass change and (e) relative wood density. Relative biomass stock and wood density were calculated as relative to the undisturbed chronosequence in the same time period

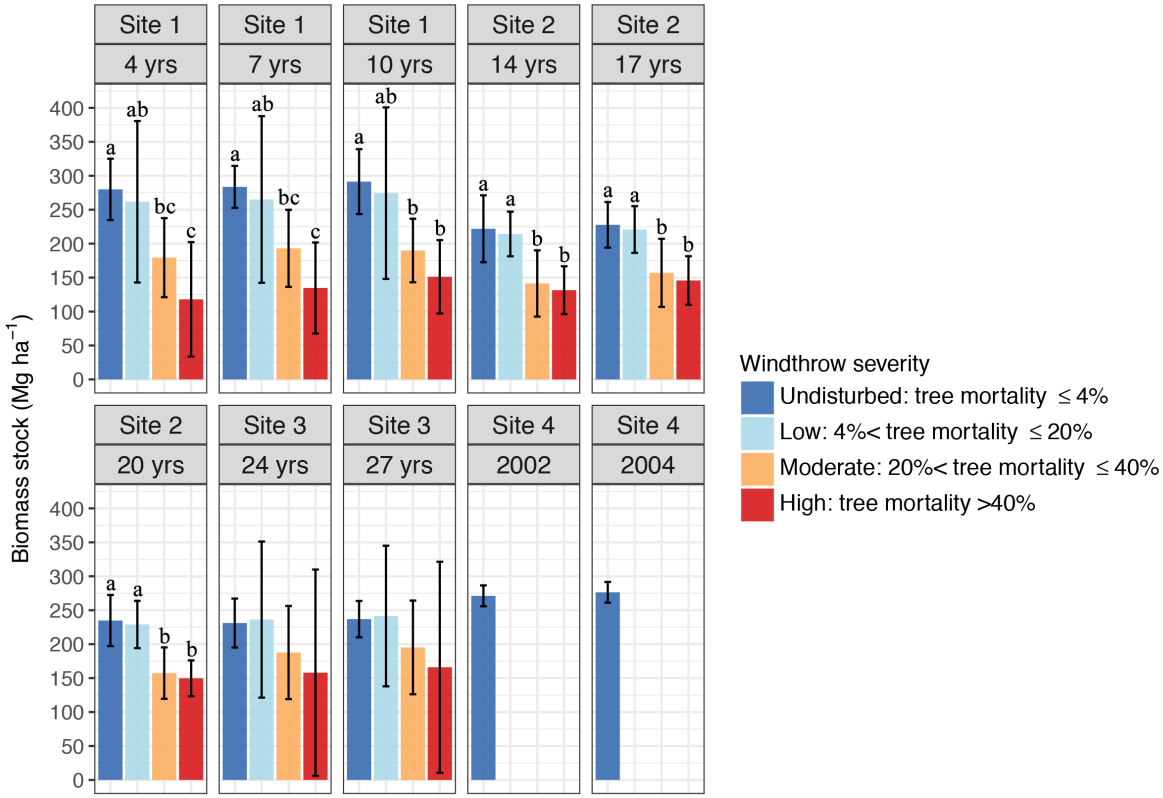

Figure S5 Biomass stock (mean±95% confidence intervals) in Central Amazon forests, Brazil. The shown data set includes old growth and wind-disturbed *terra-firme* forests that span a wide gradient of windthrow tree-mortality and 4-27 years of recovery. Different letters on top of bars denote significant differences between windthrow severities at $p < 0.05$ (for most) or $p < 0.1$ (Tukey's HSD test)

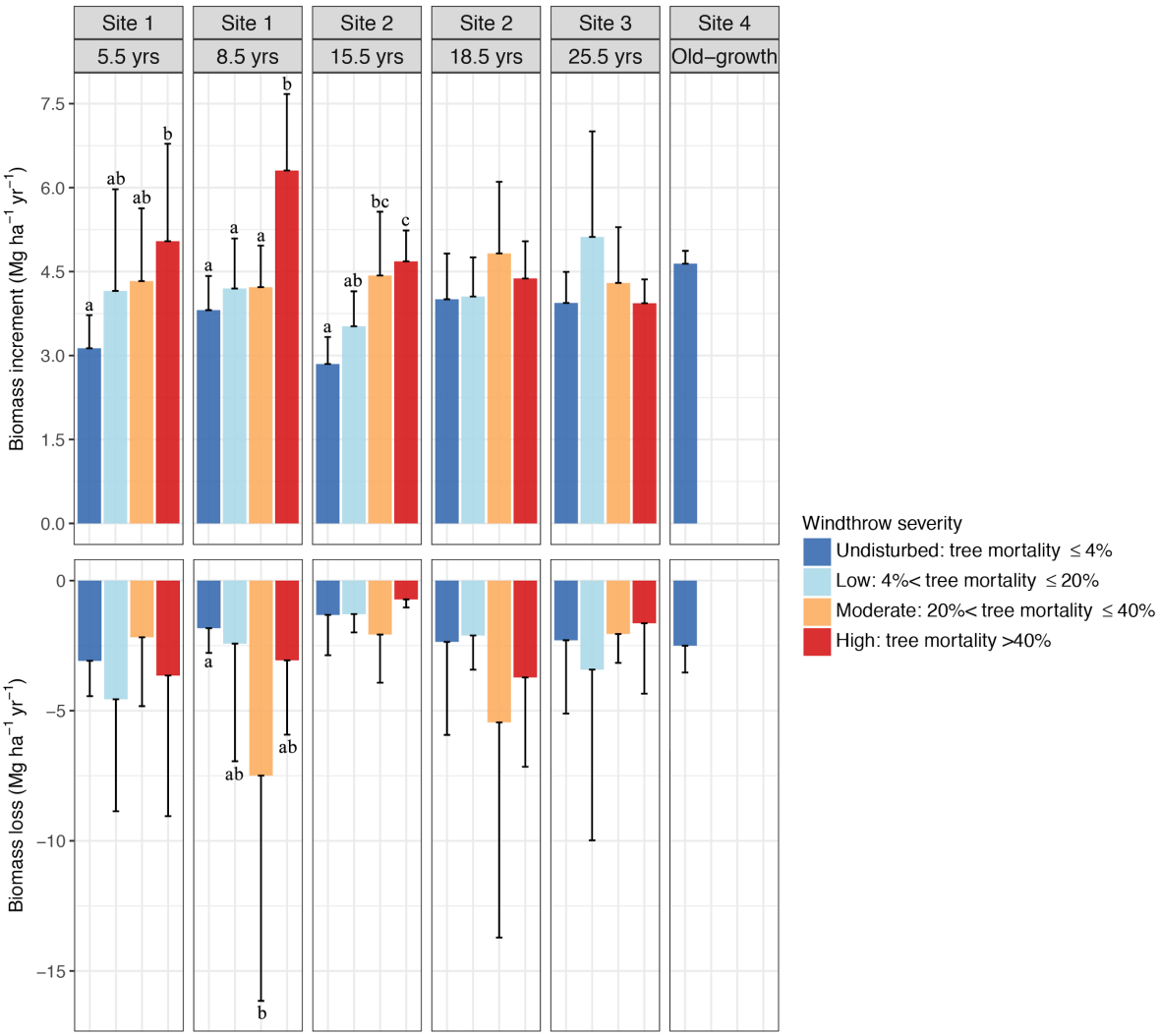

Figure S6 Biomass increment and loss (mean+95% confidence internals) in Central Amazon forests, Brazil. The shown data set includes old growth and wind-disturbed *terra-firme* forests that span a wide gradient of windthrow tree-mortality and 4-27 years of recovery. To obtain biomass increment and loss, two or three consecutive forest inventories were carried in each site. Different letters on top of bars denote significant differences between windthrow severities at $p < 0.05$ (for most) or $p < 0.1$ (Tukey's HSD test)

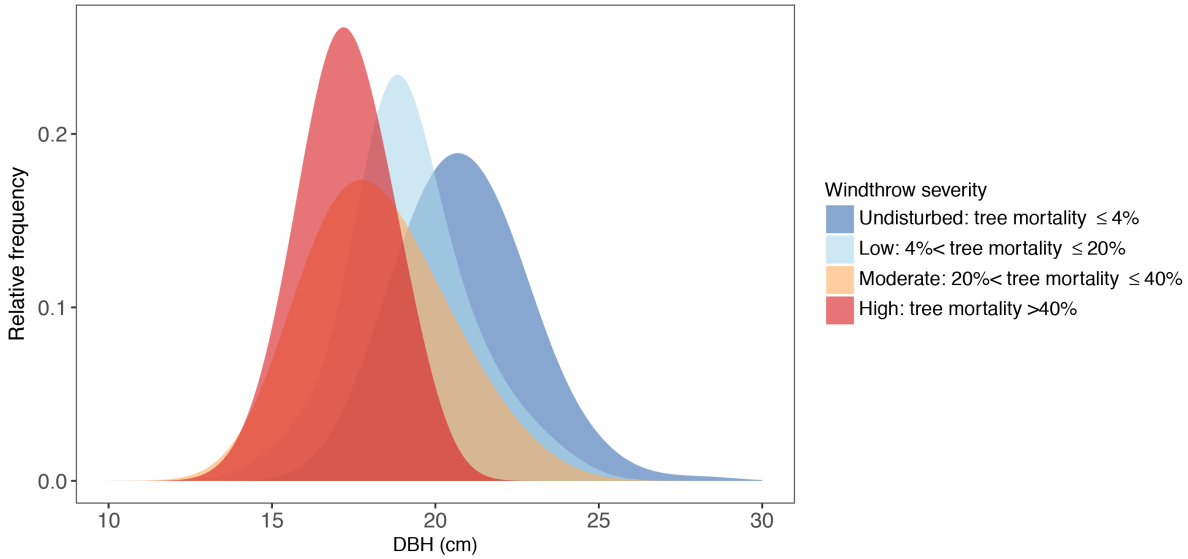

Figure S7 Size distribution of trees in Central Amazon forests, Brazil. The shown data set includes old growth and wind-disturbed *terra-firme* forests that span a wide gradient of windthrow tree-mortality and 4-27 years of recovery. Here we analyzed individual-tree data over bins of subplots with similar windthrow tree-mortality (see main text) and averaged windthrow severities over sites. The curves for windthrow severities were fit with a kernel Gaussian smoothing method resulting a symmetric and positive function that integrates to one and can be expressed as $\hat{f}_{kde}(x) = \frac{1}{n}\sum_{i=1}^{n} K\left(\frac{x-x_i}{h}\right)$, where K is the kernel and h is the bandwidth (Scott, 2015)

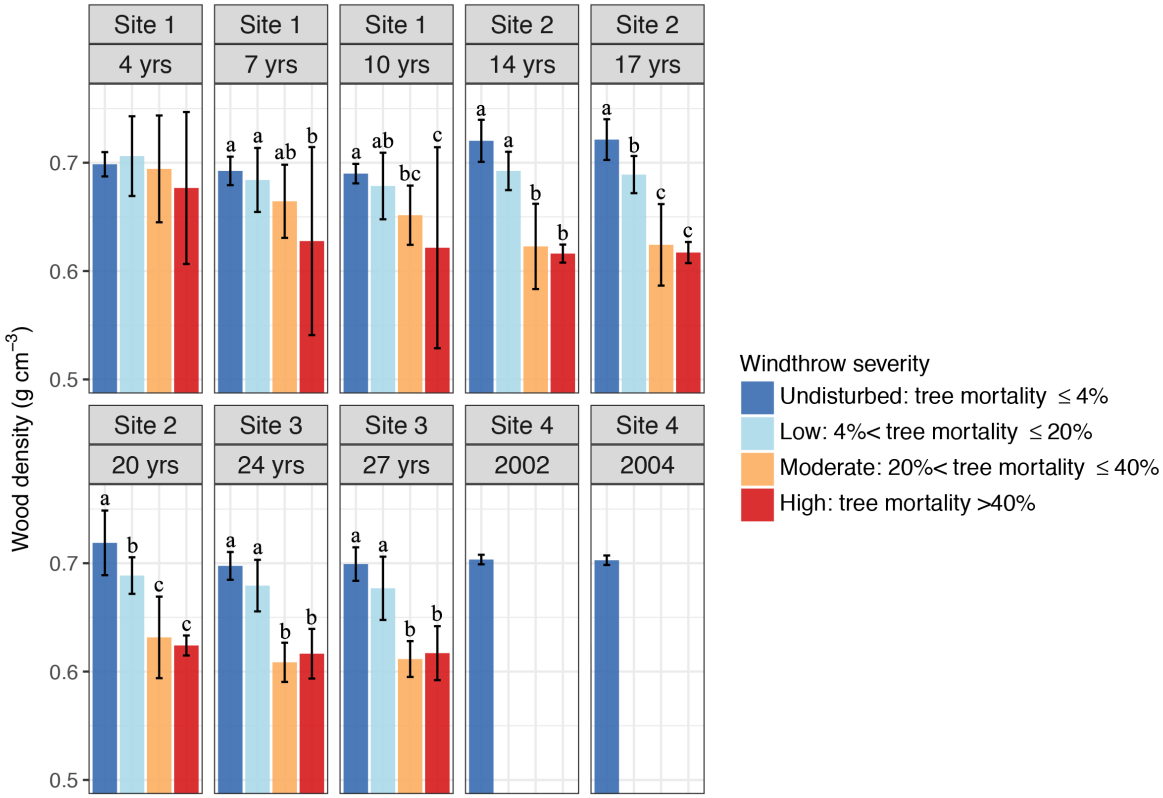

Figure S8 Wood density (mean±95% confidence internals) in Central Amazon forests, Brazil. The shown data set includes old growth and wind-disturbed *terra-firme* forests that span a wide gradient of windthrow tree-mortality and 4-27 years of recovery. Different letters on top of bars denote significant differences between windthrow severities at p <0.05 (for most) or p <0.1 (Tukey's HSD test)

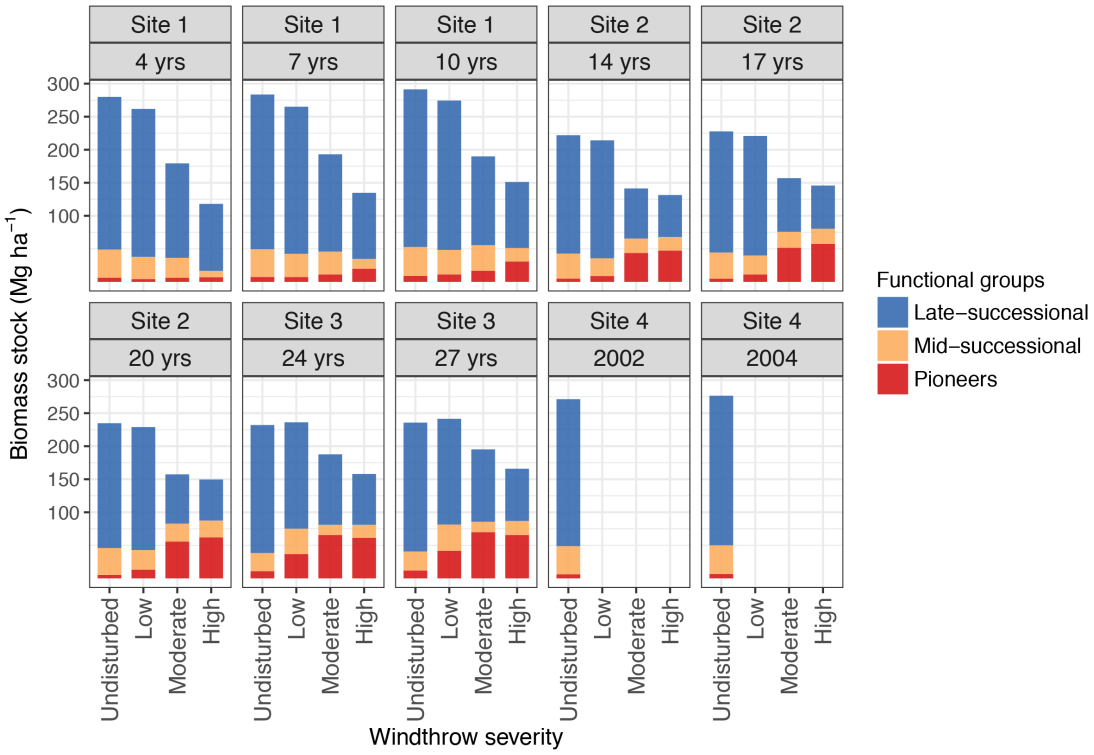

Figure S9 Biomass partitioning among functional groups in Central Amazon forests, Brazil. The shown data set includes old growth and wind-disturbed *terra-firme* forests that span a wide gradient of windthrow tree-mortality and 4-27 years of recovery. Windthrow severity: Undisturbed- windthrow tree-mortality ≤4%; Low- 4-20%; Moderate- 20-40%; High- >40%

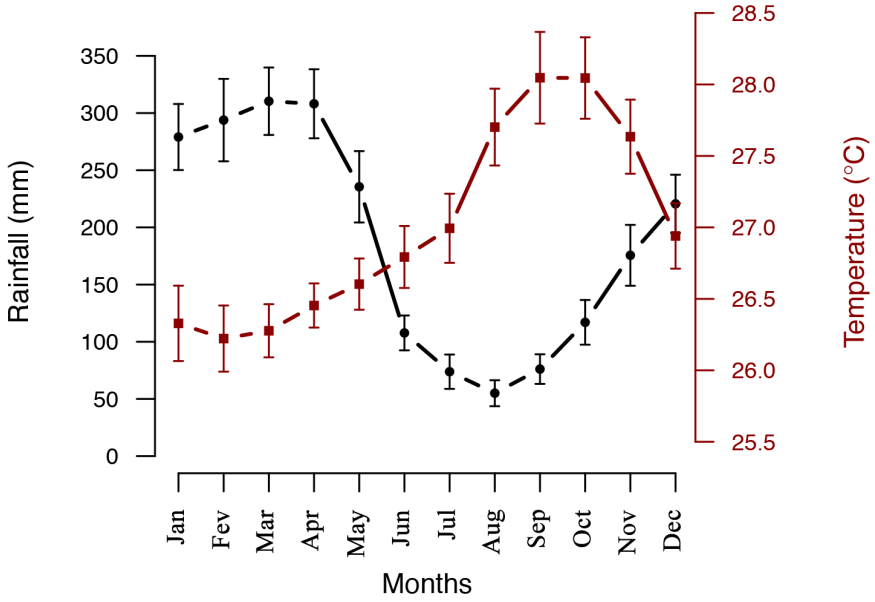

Figure S10 Climatology (based period 1970-2016) of rainfall and temperature (mean±95% confidence intervals) in Manaus, Brazil (less than 90 km distant from our study sites). Data obtained from the *Instituto Nacional de Meteorologia* (INMET; http://www.inmet.gov.br)